Imaging with spatio-temporal modelling to characterize the dynamics of plant-pathogen lesions

Melen Leclerc*[1], Stéphane Jumel[1], Frédéric M. Hamelin[1], Rémi Treilhaud[1], Nicolas Parisey[1], and Youcef Mammeri[2]

[1]IGEPP, INRAE, Institut Agro, Rennes 1 University, Rennes, France
[2]LAMFA, CNRS, Picardie Jules Verne University, Amiens, France

* Corresponding author
melen.leclerc@inrae.fr, stephane.jumel@inrae.fr, frederic.hamelin@agrocampus-ouest.fr, rtreilhaud@live.fr, nicolas.parisey@inrae.fr, youcef.mammeri@u-picardie.fr

Abstract

- Within-host spread of pathogens is an important process for the study of plant-pathogen interactions. However, the development of plant-pathogen lesions remains practically difficult to characterize and quantify beyond the common traits such as lesion area. We tackle the spatio-temporal dynamics of interactions by combining image-based phenotyping with mathematical modelling.
- We consider the spread of *Peyronellaea pinodes* on pea stipules that were monitored daily with visible imaging. We assume that pathogen propagation on host-tissues can be described by the Fisher-KPP model where lesion spread depends on both a logistic local growth and an homogeneous diffusion. Model parameters are estimated using a variational data assimilation approach on sets of registered images.
- This modelling framework is used to compare the spread of an aggressive isolate on two pea cultivars with contrasted levels of partial resistance. We show that the expected slower spread on the most resistant cultivar is actually due to a decrease of diffusion and, to a lesser extent, local growth.
- These results demonstrate that spatial models with imaging allows one to disentangle the processes involved in host-pathogen interactions. Hence, promoting model-based phenotyping of interactions would allow a better identification of quantitative traits thereafter used in genetics and ecological studies.

keywords: aggressiveness traits, ascochyta blight of pea, Fisher-KPP, disease phenotyping, computer vision, variational optimization

1 Introduction

Assessing life-history traits of pathogen on host plants is central to understand the adaptation of pathogens to plant resistance and to determine quantitative trait loci for both host resistance and pathogen aggressiveness (Lannou, 2012). The quantitative traits of host-pathogen interaction the most frequently measured are incubation and latency periods, spore production and lesion size (Pariaud et al., 2009). In practice, they are often obtained after inoculating host, monitoring the development of the lesions caused by the pathogen and finally estimating the traits of interest. However, in practice, phenotyping the dynamics of host-pathogen interactions remains challenging and is often performed through inaccurate traits that, though they already contrast phenotypes, poorly describe the processes and can hide or skew differences between individuals (Leclerc et al., 2019). The lesion size is a good example to illustrate this as there are an infinity of spatial dynamics than can produce identical size at a given time. Considering the lesion growth rate is more informative but again, it ignores lesions shapes and depends on processes such as the local growth and the diffusion. Mechanistic models offer a mean to decipher the processes involved in host-pathogen interactions but are still seldom considered for analyzing plant disease phenotypic data (Leonard and Mundt, 1984; Leclerc et al., 2019). In this case the model should remain parsimonious enough so that the parameters can be identified from the data.

The recent development of image-based phenotyping methods enables *in vivo* non-destructive longitudinal monitoring of infected tissues. Besides allowing precise and automated quantification of necrotic plant tissues, that already improved disease phenotyping (e.g Karisto et al., 2018; Bousset et al., 2019; Yates et al., 2019), imaging opens new possibilities to further investigate the spatial dimension of host-pathogen interactions. As illustrated by works on the development of human lesions, imaging data can be particularly interesting for fitting spatially explicit process-based models (Hogea et al., 2008; Mang et al., 2020). It provides new insights into the main mechanisms involved in lesion development in relation with host immunity but also modelling tools for phenotyping. Perhaps surprisingly, although the main physiological mechanisms of plants and their parasites have been described by mathematical models (e.g Boswell et al., 2003; Sellier and Mammeri, 2019) the spread of lesions has received little attention by modellers (Powell et al., 2005; Mammeri et al., 2010; Garin et al., 2014; Leclerc et al., 2019) and rarely validated against images (Belin et al., 2015).

In this study we consider the fungal pathogen *Peyronellaea pinodes* (formerly *Mycosphaerella pinodes and Didymella pinodes*) on pea as an example pathosystem to analyze its spread with modelling and imaging. With the two fungi *Phoma medicaginis* and *Ascochyta pisi*, *P. pinodes* belongs to the As-

cochyta blight of pea disease complex that causes substantial yield losses worldwide (Bretag et al., 2006). In Europe, *P. pinodes* is generally the predominant and the most destructive species, though *P. medicaginis* is also prevalent and tends to develop later in the growing season (Dutt et al., 2020, 2021). *P. pinodes* is able to infect all aerial parts of its host plant and induces necrotic growing lesions. The development of resistant cultivars to *P. pinodes* has been central for the integrated management of this disease, but difficult as only quantitative (or partial) resistance was available (Prioul et al., 2004; Bretag et al., 2006). For most fungal pathogens, quantitative host resistance alters spore production and infection as well as within-host growth (Pariaud et al., 2009; Lannou, 2012; Leclerc et al., 2019). The evaluation of quantitative host resistance on pathogen life-history traits is often performed in controlled conditions with *ad hoc* protocols. In the case of *P. pinodes* partial resistance of pea can be assessed on inoculated detached leaflets, or stipules, by measuring necrotic lesions either manually (Onfroy et al., 2007) or with imaging (Dutt et al., 2020).

We begin by presenting the experiment, including the image acquisition protocol and the processing framework, that allowed the longitudinal monitoring of lesions on inoculated pea stipules. Then, we consider the Fisher-KPP reaction-diffusion model to describe the spread of necrotic lesions on host tissues which is fitted to image sequences. We show that combining imaging and spatially explicit models enables a finer description of within-host spread of pathogen, including lesions coalescence, and allows one to disentangle local growth and diffusion of the necrosis. The comparison of estimated parameters obtained on two cultivars provides new insights into the effects of host quantitative resistance on lesion spread. We finish by discussing our work and how further developments inspired from biomedical research may contribute to improve our understanding of host-pathogen interactions and provide mathematical tools for precision phenotyping.

2 Materials and methods

2.1 Host inoculation experiment

The aggressive isolate of *P. pinodes* named *Mp 91.31.12* was inoculated on two pea cultivars previously tested in our laboratory: Solara, a common susceptible reference, and James, that reduces symptom development in controlled conditions (Onfroy et al., 2007). These two cultivars are semi-leafless without conventional leaves but extended pairs of hypertrophied stipules below each stem node. For each cultivar, leaf stipules were inoculated according to a standard biotest protocol developed in our laboratory (Onfroy et al., 2007; Dutt et al., 2020). Plants were grown in a climate chamber, kept at 18°C and with a 12h photoperiod, in 9cm diameter pots containing vermiculite and five pea seeds. When they reached the 6 leaf stage, stipules from nodes 3 and 4 were sampled and placed on tap water in a compartmented square Petri dish. The inoculum consisted in a pycnidiospore suspension whose concentration was de-

termined with a haemocytometer and adjusted at 5×10^4 spores ml^{-1} following Onfroy et al. (2007) protocol. For both cultivar, 32 pairs of attached stipules were inoculated by placing a 10μl droplet at their center. Afterwards, the Petri dishes containing the inoculated stipules were placed into transparent plastic containers to avoid drop evaporation and incubated in a climatic chamber kept at 20°C and with a 14 h photoperiod.

2.2 Image acquisition

The spread of lesions caused by the pathogen was assessed daily from 3 to 7 days after inoculation (Fig.1) following a standardized acquisition protocol developed for plant disease phenotyping (Bousset et al., 2019; Dutt et al., 2020). Image acquisition was performed using two FotoQuantum LightPro 50 × 70 cm soft boxes, placed on both sides of the Petri dish with four daylight bulbs each (5400 K, 30 W). Pictures were taken with a Nikon D5300 digital camera equipped with an AF-S DX Micro Nikkor 40 mm 1:2.8G lens, on a Kaiser Repro stand, and with computer control using DigiCamControl software ver. 2.1.1.0. Aperture was set at F22 for maximal depth of field, iso 125, daylight white balance. Initial pictures were saved as RGB images with a resolution of 6000 × 4000 pixels.

2.3 Image processing

As illustrated in Figure 1, several processing steps were required to enable model fitting to image sequences. First, stipules (i.e. our region of interest) were extracted from raw images using the Simple Interactive Object Extraction algorithm (Friedland et al., 2005) (Fig.1a). Second, images were registered (i.e. aligned to each other) using the Coherent Point Drift method (Myronenko and Song, 2010), assuming rigid transformations and the first image (3 days after inoculation) as the reference (Fig.1b). Third, images were segmented by classifying pixels in either healthy, symptomatic or background classes. The prediction of each pixel-class was based on several nonlinear image features that captured local image characteristics. In particular we computed features for colours and noise (e.g. Gaussian blur), edges (e.g. Laplacian), and textures (eigenvalues of tensor structure and hessian) at different scales using spherical filters with radii varying from 1 to 16 pixels. Based on these features, Random Forest classifiers were trained for each date of observation using the Trainable Waikato Environment for Knowledge Analysis (Weka) (Arganda-Carreras et al., 2017). They were tested on ground truth images from an independent study (Dutt et al., 2020) and showed good performances to classify pixels (Table S1). Afterwards, these classifiers were used to process the full dataset and to get three probability maps giving the probabilities of each pixel to be in each class (Fig.1c). To finish with, we considered the Jaccard index (i.e. the intersection over the union of the two sets, that can vary between 0 and 100%) as a measure of stipules deformation, that was computed for each date assuming the 3rd day as the reference set.

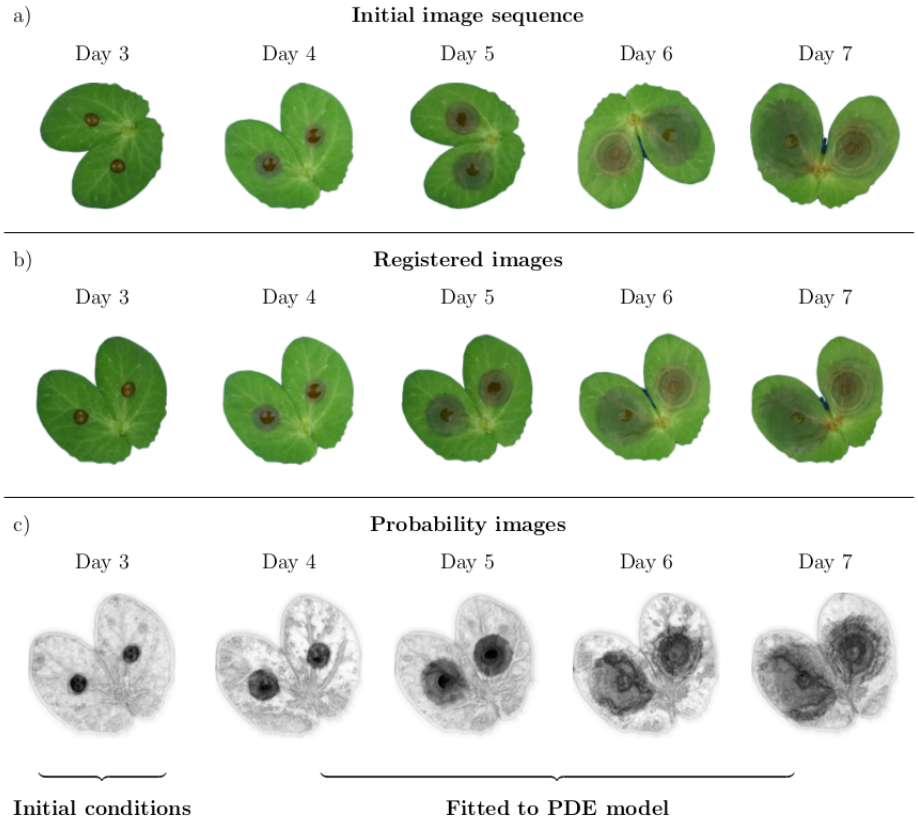

Figure 1: Schematic representation of lesion growth monitoring through imaging. The initial RGB images (a) are first registered to align stipules in time (b). Afterwards, a supervised segmentation is performed to produce probability maps indicating the probability of each pixel to be in either healthy, symptomatic or background classes. Probability images of the symptomatic class (c) are used for fitting the Fisher-KPP model. Images of day 3 are used as initial conditions while the remaining 4 images are used to estimate the pathogen local growth rate $\hat{a}$ and diffusion coefficient $\hat{D}$ that are actually two distinct life-history traits of within-host pathogen spread.

2.4 Spatial lesion growth model

Most existing models for the spread of plant pathogens within host tissues are rather spatially implicit and generally assume a constant radial growth rate and a simplified geometry of the host organ (Powell et al., 2005; Mammeri et al., 2010; Garin et al., 2014). Yet, these models were able to fit non-spatial lesion size data (Leclerc et al., 2019), including for the particular *P. pinodes*-pea pathosystem (Dutt et al., 2020). Here, we consider the Fisher-KPP model to describe the spatially explicit spread of the pathogen on host tissues. The Fisher-KPP equation was introduced in 1937 by Fisher (Fisher, 1937) and Kolmogorov-Petrovsky-Piskunov (Kolmogorov et al., 1937) as a semilinear parabolic partial differential equation (PDE) combining Fick's diffusion with logistic growth. Let $\Omega \in \mathbb{R}^2$ be the stipules area. The Fisher-KPP equation reads as the following reaction-diffusion equation, for the position $\mathbf{x} = (x, y) \in \Omega$ and the time $t > 0$

$$\frac{\partial u}{\partial t}(\mathbf{x}, t) = D\Delta u(\mathbf{x}, t) + au(\mathbf{x}, t)\left(1 - \frac{u(\mathbf{x}, t)}{K}\right). \tag{1}$$

where $u(\mathbf{x}, t)$ denotes the local density of pathogen mycelium, $D > 0$ is the diffusion coefficient, $a \geq 0$ the local growth rate of the mycelium, and $K > 0$ its maximum local biomass. The equation is closed thanks to a given initial image u_0 as

$$u(\mathbf{x}, t = t_3) = u_0(\mathbf{x}) \text{ in } \Omega.$$

Assuming the pathogen cannot move out of the leaf, homogeneous Neumann boundary conditions are imposed

$$\frac{\partial u}{\partial n}(\mathbf{x}, t) = 0 \text{ on } \partial\Omega.$$

This model exhibits traveling waves with asymptotic speed $2\sqrt{aD}$ which is coherent with the assumption of a constant radial growth rate considered in several studies and supported by non-spatial lesion data.

Numerical solutions of the model are obtained by computing the spatial domain Ω with a level-set formalism so the boundaries $\partial\Omega$ match those of the leaves in the image (Osher and Fedkiw, 2002; Sethian, 1999), and solving the partial differential equations using explicit Euler finite differences in time and second order centered finite differences in space. More details on these numerical aspects are provided in supplementary information S2.

2.5 Parameters estimation from image sequences

For each inoculated stipule, the observations consisted in a set of registered images $u_{reg}(\mathbf{x}, \mathbf{t})$ for times after inoculation $\mathbf{t} = \{t_3, t_4, t_5, t_6, t_7\}$ (Fig. 1). Parameters identification consisted in seeking estimates $\hat{\theta}$ such that the output of the spatial model $u(\mathbf{x}, t, \theta)$ matches these observations. Depending on the estimation problem, inverse problems or statistical inference of reaction-diffusion can be addressed by several methods such as mathematical analysis, maximum

likelihood or non-linear least-squares (Soubeyrand and Roques, 2014). When observations are image sequences it is more relevant to rely on data assimilation methods that have been developed and used to fit models in fluid dynamics (Papadakis and Mémin, 2008) or biomedical modelling (Mang et al., 2020). We consider a variational data assimilation approach based on optimal control theory (Asch et al., 2016). The estimation procedure is based on the nonlinear least-squares cost function:

$$J(\theta) = \frac{1}{2} \int_{t_3}^{t_7} \int_{\Omega} (u(\mathbf{x}, t, \theta) - u_{reg}(\mathbf{x}, t))^2 d\mathbf{x}dt \tag{2}$$

Following the variational assimilation framework (Asch et al., 2016), estimates $\hat{\theta}$ are found by minimizing $J(\theta)$ thanks to the Lagrangian function $\mathcal{L}(\theta)$ and a numerical procedure both detailed in appendix S2.2.

In practice, we considered the probability images, predicted by the supervised classifiers, instead of the RGB images as observations $u_{reg}(\mathbf{x}, \mathbf{t})$ (Hogea et al., 2008). This allowed us to set $K = 1$ and only estimate the local growth rate a and the diffusion coefficient D. For each image sequence, the image of the 3rd day is set as the initial conditions $u_0(\mathbf{x})$, and the remaining 4 images are used for data assimilation. As the diffusion coefficient depends on image size, we rather considered the relative diffusion, i.e. the raw diffusion coefficient divided by stipules area (SI S2.3). The model was fitted to the 2×16 inoculated stipules and we compared the two cultivars through one-way ANOVAs on both the local growth rate and the diffusion coefficient. The adequacy of the Fisher-KPP model to the data was assessed visually by looking at the raw residuals.

3 Results

The Fisher-KPP model and its numerical resolution were able to describe the spread and the coalescence of lesions caused by *P. pinodes* on pea stipules as observed in standard biotests (Fig.2, Movies S1-2, S2.3). The image processing framework associated with the data assimilation method allowed us to fit the reaction-diffusion model that captured the essential patterns of the spatio-temporal data. Overall, the visual assessment of raw residuals distributions points out a good centering with an increasing heteroscedasticity and a negative skewness with time (Figs. S2-3). This pattern might be explained by a slight tendency of the model to underestimate lesion spread and the continuous change of stipules shape associated with errors during images registration. Although stipules deformation remained limited with Jaccard indexes above 80 for all individuals (Fig.3), it may have induced some bias in the alignment of lesions as illustrated in Figure 2b at day 7.

We successfully estimated the local growth rate and the diffusion coefficient for the 32 monitored individuals (Table S3). The James cultivar was characterized by smaller stipules than Solara with average surfaces of 4.49 and 7.93 cm^2 respectively. The comparison of estimated parameters between cultivars

suggested that quantitative resistance significantly reduced the diffusion coefficient and, to a lesser extent, the local growth rate (p-values < 0.05, Table S4), for which the distribution of estimates have higher overlap between cultivars (Fig.3). The cultivar James had indeed mean estimated growth rate $\hat{a}$ and diffusion coefficient $\hat{D}$ of respectively 0.496 and 0.291 against 0.536 and 0.489 for the more susceptible cultivar Solara. These results suggest that, for inoculated stipules with identical areas and shapes, lesions caused by *P. pinodes* will spread at a higher speed, and thus coalesce and reach edges earlier, on Solara than on James (Fig.2). This is consistent with previous results based on the comparison of cultivars through lesions areas without disentangling pathogen diffusion and local growth.

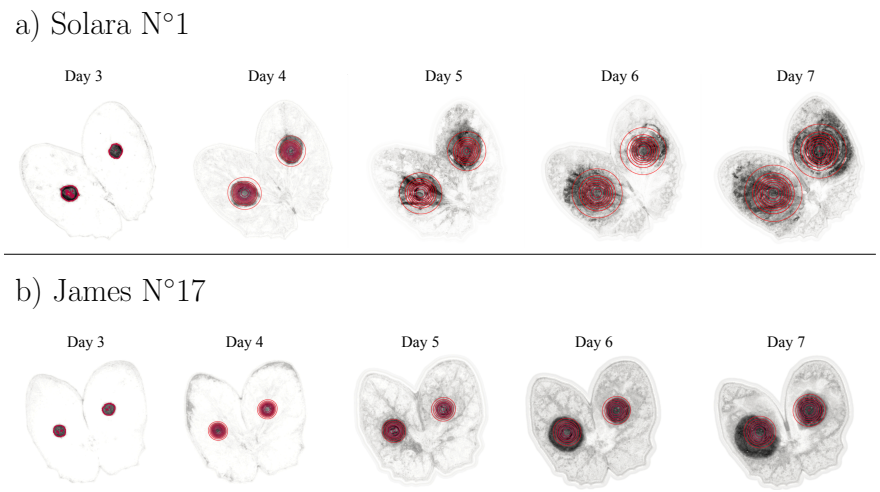

Figure 2: Visualization of model prediction against image data. The solution of the fitted Fisher-KPP equation, i.e. with optimal estimated parameters, is represented through time by contours $(0.1, 0.2, \ldots, 1)$ overlying the probability image sequences of the symptomatic class for example stipules of Solara (a) et James (b) cultivars. This comparison between the spatial model and the data is also available in two movies provided as supplementary materials (Movies S1-S2).

4 Discussion

In this study we combined image processing and mathematical modelling to investigate the dynamics of host-pathogen interactions. We showed that a longitudinal monitoring of inoculated leaves through visible imaging provides

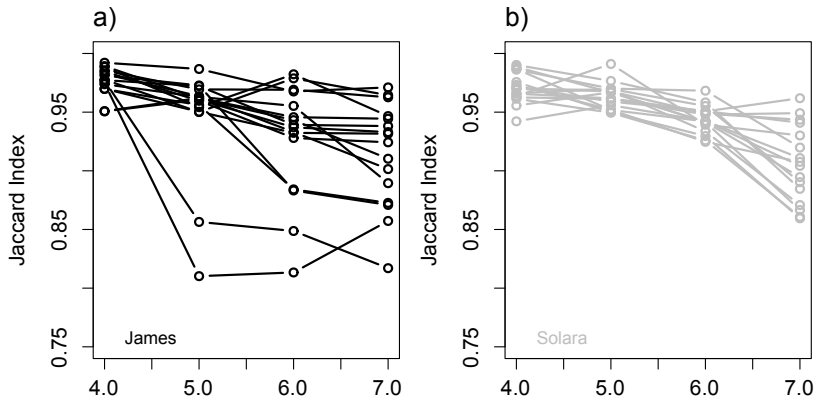

Figure 3: Visualization of stipules deformation in time. Change in the Jaccard index with time for cultivars James (a) and Solara (b). At each time after inoculation the Jaccard index was calculated in comparison with the image at day 3, also used as a reference for image registration.

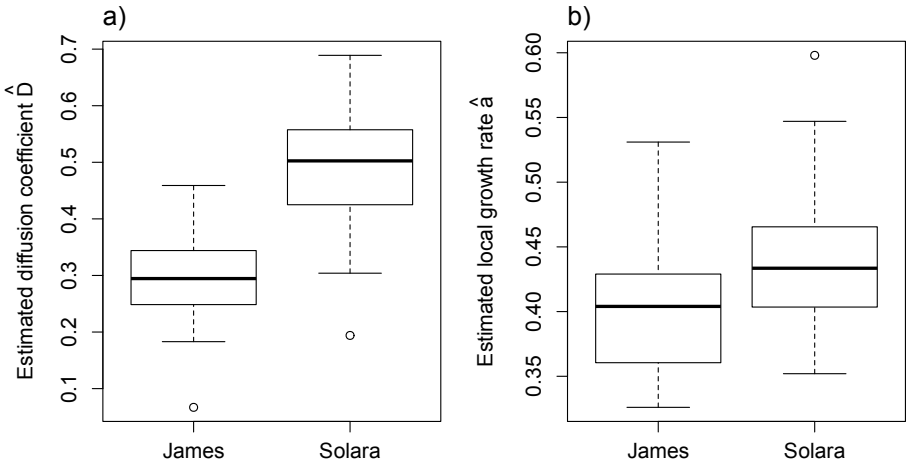

Figure 4: Distributions of the estimated parameters. a) diffusion coefficient $\hat{D}$ with a mean values of 0.291 for James against 0.489 for the more resistant cultivar Solara, b) local growth rate $\hat{a}$ with mean values of 0.496 and 0.536 for respectively James and Solara. All estimated coefficient are available in supplementary information (Table S3).

data to fit reaction-diffusion models that describe the spatio-temporal spread of pathogen on host tissues. While such methodological approaches are common in biomedical sciences (e.g Mang et al., 2020) they are original in plant pathology. Here, we considered the fungal pathogen *P. pinodes* on pea as an example pathosystem and used the Fisher-KPP equation to model necrotrophic lesions. Using this PDE model with a variational data assimilation method we were able to capture the essential patterns of image-sequences data and disentangle local growth and diffusion. These processes are actually two distinct life-history traits that both explain host colonization by the pathogen through lesions. They provide a finer description of the interaction but cannot be determined without the use of spatially-explicit models with spatial information, as provided by images, as different local growth and diffusion can lead to identical lesion speed. Furthermore, while lesions coalescence, different leaves sizes, or lesion saturation at leaves boundaries can be problematic when comparing lesion sizes in common aggressiveness biotests, the inference of parameters in parsimonious PDE models can handle properly such situations.

We assessed the development of an aggressive isolate on two cultivars with contrasted level of partial resistance using a standard protocol developed for screening both pathogen aggressiveness and host resistance (Onfroy et al., 2007). Our results were consistent with previous findings as the spread of lesions caused by *P. pinodes* was slower on James than Solara. Most interestingly, we demonstrated that quantitative host resistance decreased significantly pathogen diffusion and, to a lesser extent, its local growth rate. Of course these effects should be further confirmed on a larger panel of pathogen isolates and host genotypes. Yet, although such effects may not be surprising they cannot be identified and quantified through usual aggressiveness data without the use of spatial models and data. This illustrates well how combining advanced imaging methods and mechanistic models can help to improve the comparison of cultivars (or isolates) and gain new insights into host resistance to disease. Optical sensors recently percolated in plant sciences and contributed to recent development of precision phenotyping for plant diseases (Mahlein, 2016; Karisto et al., 2018; Yates et al., 2019). On the other side the usefulness of mechanistic models for analyzing phenotypic data is recognized (e.g. Leonard and Mundt, 1984; Leclerc et al., 2019) but remains seldom considered. We think that promoting the use of mechanistic models for processing precision phenotyping data would be particularly relevant for assessing the genetic architecture of traits, either for the plant or the pathogen, understand pathogen adaptation to plant resistance and develop new cultivars.

Although our modelling framework was able to describe the visible spread of nectrotrophic lesions caused by *P. pinodes* and provides original knowledge on this pathosystem, it may be improved and extended on several points. Firstly, for the sake of simplicity we ignored stipules deformation. This change in the shape of host organs caused by parasitism frequently occurs in plants and would be worth considering using existing mathematical and numerical methods for explicit modelling of shapes (Osher and Fedkiw, 2002) or plant growth (Bonneu et al., 2012). While such improvement would increase the complexity of the

model, it may contribute to decrease the discrepancy between the model and the data, and perhaps, help to identify genotypes that are less susceptible to disease-induced deformation. Secondly, the inoculated host leaves were digitalized through visible imaging and the reaction-diffusion model was fitted to probability maps obtained with trained classifiers (Hogea et al., 2008). Therefore, by doing so we assumed that lesions appearances over time, learned by experts, were directly related to pathogen density. It would also be possible to combine different signals that are correlated with pathogen load considering multimodal imaging (Belin et al., 2013), or to fit the model by considering only the predicted edges of lesions (i.e. binary data). However, there will always be an uncertainty on the appearance and observation models that could only be further validated by quantifying pathogen density with complementary measurements like real-time quantitative PCR. Thirdly, as lesions caused by *P. pinodes* appeared to spread at a constant speed with quite homogeneous patterns we choose the Fisher-KPP model to describe the spatial dynamics. However, this model may not be appropriate to describe the spreading processes that occur in all pathosystems. The spatial dynamics of plant-pathogen lesions remains poorly addressed and further works could benefit from theoretical knowledge on PDE for propagating systems and existing models for the spread of invasive organisms (Mammeri et al., 2014; Roques and Bonnefon, 2016), microbial populations and fungal colonies (Boswell et al., 2003), or human lesions (Hogea et al., 2008; Mang et al., 2020). For instance, the effect of leaf veins that can orientate lesion spread in some pathosystems could be considered through advection terms or by considering hybrid reaction-diffusion models with different dynamics on host tissues (2D) and veins (1D) (Roques and Bonnefon, 2016). On the other side, like microbial populations in controlled media, plant-pathogen lseions can be interesting experimental systems to test and feed some mathematical theories (Müller et al., 2014). Fourthly, our model ignored any host response to infection and further development could take into account some key physiological and immune processes. For instance it would be worth including ontogenetic and disease-induced changes in host susceptibility, e.g. caused by senescence or hypersensitive responses, that are known to occur in several pathosystems and can be spatially localized on leaf tissues (Dolatabadian et al., 2020; Richard et al., 2012).

From an epidemiological point of view the within-host dynamics of the pathogen is an important phase that can have strong impact on epidemics at the population level. Scaling-up the behaviour of epidemics from individuals to populations is still a difficult question for mathematical and computational epidemiology and, at least in the case of plant diseases, the within-host spread of pathogens is either ignored or extremely simplified compared to other epidemiological processes such as spores production (Segarra et al., 2001; Powell et al., 2005; Garin et al., 2014; Mammeri et al., 2014). This is mainly due to the challenges of multiscale and spatial modelling, but perhaps, also to the lack of spatial models for within-host pathogen development. Thus, we believe that besides providing new fundamental knowledge and phenotyping tools, spatial lesions models that describe observable spread of pathogen on host organs

would also contribute to improve modelling works focused on higher scales. In addition, new insights into the effects of host resistance on within-host dynamics would also feed models for understanding the durability plant resistance to diseases (Bourget et al., 2015; Fabre et al., 2021; Rimbaud et al., 2021). For instance, the impact of partial resistance on either the diffusion coefficient or the local growth rate may affect differently pathogen fitness and have contrasted impacts on pathogen invasion, persistence and evolution.

5 Acknowledgements

This study was part of the StartIRM project funded by the Université Bretagne Loire. We thank Alain Baranger, Christophe Le May, Agathe Dutt, Lydia Bousset and Tristan Boureau for useful discussions, and Claudine Pasco and Amélie Morin for their help during the experiment.

References

Arganda-Carreras, I., Kaynig, V., Rueden, C., Eliceiri, K.W., Schindelin, J., Cardona, A., Sebastian Seung, H., 2017. Trainable weka segmentation: a machine learning tool for microscopy pixel classification. Bioinformatics 33, 2424–2426.

Asch, M., Bocquet, M., Nodet, M., 2016. Data assimilation: methods, algorithms, and applications. SIAM.

Belin, E., Chapeau-Blondeau, F., Rousseau, D., 2015. Modèle stochastique et représentation par graphe pour le suivi spatio-temporel de pathogènes à la surface de feuilles par imagerie, in: 25ème Colloque GRETSI sur le Traitement du Signal et des Images, p. 4.

Belin, É., Rousseau, D., Boureau, T., Caffier, V., 2013. Thermography versus chlorophyll fluorescence imaging for detection and quantification of apple scab. Computers and electronics in agriculture 90, 159–163.

Bonneu, A., Dumont, Y., Rey, H., Jourdan, C., Fourcaud, T., 2012. A minimal continuous model for simulating growth and development of plant root systems. Plant and soil 354, 211–227.

Boswell, G.P., Jacobs, H., Davidson, F.A., Gadd, G.M., Ritz, K., 2003. Growth and function of fungal mycelia in heterogeneous environments. Bulletin of Mathematical Biology 65, 447–477.

Bourget, R., Chaumont, L., Durel, C.E., Sapoukhina, N., 2015. Sustainable deployment of qtls conferring quantitative resistance to crops: first lessons from a stochastic model. New Phytologist 206, 1163–1171.

Bousset, L., Palerme, M., Leclerc, M., Parisey, N., 2019. Automated image processing framework for analysis of the density of fruiting bodies of leptosphaeria maculans on oilseed rape stems. Plant Pathology 68, 1749–1760.

Bretag, T., Keane, P.J., Price, T., 2006. The epidemiology and control of ascochyta blight in field peas: a review. Australian Journal of Agricultural Research 57, 883–902.

Dolatabadian, A., Batley, J., Edwards, D., Barbetti, M., 2020. Virulence/avirulence patterns among leptosphaeria maculans isolates determines expression of resistance, senescence and yellowing in cotyledons of brassica napus. European Journal of Plant Pathology 156, 1077–1089.

Dutt, A., Andrivon, D., Jumel, S., Le Roy, G., Baranger, A., Leclerc, M., Le May, C., 2020. Life history traits and trade-offs between two species of the ascochyta blight disease complex of pea. Plant Pathology 69, 1108–1124.

Dutt, A., Anthony, R., Andrivon, D., Jumel, S., Le Roy, G., Baranger, A., Leclerc, M., Le May, C., 2021. Competition and facilitation among fungal plant parasites affect their life-history traits. Oikos 130, 652–667.

Fabre, F., Burie, J.b., Ducrot, A., Lion, S., Richard, Q., Djidjou-Demasse, R., 2021. An epi-evolutionary model for predicting the adaptation of spore-producing pathogens to quantitative resistance in heterogeneous environments. Evolutionary Applications .

Fisher, R., 1937. The wave of advance of an advantageous gene. Annu. Eugenics 7.

Friedland, G., Jantz, K., Rojas, R., 2005. Siox: Simple interactive object extraction in still images, in: Seventh IEEE International Symposium on Multimedia (ISM'05), IEEE. pp. 7–pp.

Garin, G., Fournier, C., Andrieu, B., Houlès, V., Robert, C., Pradal, C., 2014. A modelling framework to simulate foliar fungal epidemics using functional–structural plant models. Annals of botany 114, 795–812.

Hogea, C., Davatzikos, C., Biros, G., 2008. An image-driven parameter estimation problem for a reaction–diffusion glioma growth model with mass effects. Journal of mathematical biology 56, 793–825.

Karisto, P., Hund, A., Yu, K., Anderegg, J., Walter, A., Mascher, F., McDonald, B.A., Mikaberidze, A., 2018. Ranking quantitative resistance to septoria tritici blotch in elite wheat cultivars using automated image analysis. Phytopathology 108, 568–581.

Kolmogorov, A., Petrovsky, I., Piscounoiv, N., 1937. Etude de l'équation de la diffusion avec croissance de la quantité de la matière et son application à un problème biologique. Bull. Univ. Moscow Ser. A 1, 1–25.

Lannou, C., 2012. Variation and selection of quantitative traits in plant pathogens. Annual review of phytopathology 50, 319–338.

Leclerc, M., Clément, J.A., Andrivon, D., Hamelin, F.M., 2019. Assessing the effects of quantitative host resistance on the life-history traits of sporulating parasites with growing lesions. Proceedings of the Royal Society B 286, 20191244.

Leonard, K., Mundt, C., 1984. Methods for estimating epidemiological effects of quantitative resistance to plant diseases. Theoretical and applied genetics 67, 219–230.

Mahlein, A.K., 2016. Plant disease detection by imaging sensors–parallels and specific demands for precision agriculture and plant phenotyping. Plant disease 100, 241–251.

Mammeri, Y., Burie, J., Calonnec, A., Cokelaer, T., Costes, E., Langlais, M., Pradal, C., 2010. Modelling of the airborne dispersal of a pathogen over a structured vegetal cover, in: 6th International Workshop on Functional-Structural Plant Models, pp. 55–57.

Mammeri, Y., Burie, J.B., Langlais, M., Calonnec, A., 2014. How changes in the dynamic of crop susceptibility and cultural practices can be used to better control the spread of a fungal pathogen at the plot scale? Ecological modelling 290, 178–191.

Mang, A., Bakas, S., Subramanian, S., Davatzikos, C., Biros, G., 2020. Integrated biophysical modeling and image analysis: application to neuro-oncology. Annual review of biomedical engineering 22, 309–341.

Müller, M.J., Neugeboren, B.I., Nelson, D.R., Murray, A.W., 2014. Genetic drift opposes mutualism during spatial population expansion. Proceedings of the National Academy of Sciences 111, 1037–1042.

Myronenko, A., Song, X., 2010. Point set registration: Coherent point drift. IEEE transactions on pattern analysis and machine intelligence 32, 2262–2275.

Onfroy, C., Baranger, A., Tivoli, B., 2007. Biotic factors affecting the expression of partial resistance in pea to ascochyta blight in a detached stipule assay. European Journal of Plant Pathology 119, 13–27.

Osher, S., Fedkiw, R., 2002. Level Set Methods and Dynamic Implicit Surfaces. Springer New York.

Papadakis, N., Mémin, É., 2008. Variational assimilation of fluid motion from image sequence. SIAM Journal on Imaging Sciences 1, 343–363.

Pariaud, B., Ravigné, V., Halkett, F., Goyeau, H., Carlier, J., Lannou, C., 2009. Aggressiveness and its role in the adaptation of plant pathogens. Plant Pathology 58, 409–424.

Powell, J.A., Slapničar, I., van der Werf, W., 2005. Epidemic spread of a lesion-forming plant pathogen—analysis of a mechanistic model with infinite age structure. Linear Algebra and its Applications 398, 117–140.

Prioul, S., Frankewitz, A., Deniot, G., Morin, G., Baranger, A., 2004. Mapping of quantitative trait loci for partial resistance to mycosphaerella pinodes in pea (pisum sativum l.), at the seedling and adult plant stages. Theoretical and Applied Genetics 108, 1322–1334.

Richard, B., Jumel, S., Rouault, F., Tivoli, B., 2012. Influence of plant stage and organ age on the receptivity of pisum sativum to mycosphaerella pinodes. European Journal of Plant Pathology 132, 367–379.

Rimbaud, L., Fabre, F., Papaïx, J., Moury, B., Lannou, C., Barrett, L.G., Thrall, P.H., 2021. Models of plant resistance deployment. Annual Review of Phytopathology 59.

Roques, L., Bonnefon, O., 2016. Modelling population dynamics in realistic landscapes with linear elements: A mechanistic-statistical reaction-diffusion approach. PloS one 11, e0151217.

Segarra, J., Jeger, M., Van den Bosch, F., 2001. Epidemic dynamics and patterns of plant diseases. Phytopathology 91, 1001–1010.

Sellier, D., Mammeri, Y., 2019. Diurnal dynamics of phloem loading: theoretical consequences for transport efficiency and flow characteristics. Tree physiology 39, 300–311.

Sethian, J., 1999. Level Set Methods and Fast Marching Methods: Evolving Interfaces in Computational Geometry, Fluid Mechanics, Computer Vision, and Materials Science. Cambridge University Press.

Soubeyrand, S., Roques, L., 2014. Parameter estimation for reaction-diffusion models of biological invasions. Population ecology 56, 427–434.

Yates, S., Mikaberidze, A., Krattinger, S.G., Abrouk, M., Hund, A., Yu, K., Studer, B., Fouche, S., Meile, L., Pereira, D., et al., 2019. Precision phenotyping reveals novel loci for quantitative resistance to septoria tritici blotch. Plant phenomics 2019.